

ASSESSMENT OF THE POSSIBILITY OF FOAM GLASS APPLICATION IN THE SUB-BALLAST LAYERS

Libor IŽVOLT¹, Peter DOBEŠ¹, Michaela HOLEŠOVÁ², Deividas NAVIKAS^{3,4*}

¹Department of Railway Engineering and Track Management, Univesity of Žilina, Žilina, Slovakia

²Department of Structural Mechanics and Applied Mathematics, Univesity of Žilina, Žilina, Slovakia

³Department of Mobile Machinery and Railway Transport, Vilnius Gediminas Technical University,
Vilnius, Lithuania

⁴Department of Automobiles Transport Engineering, Vilnius Technology and Design College,
Vilnius, Lithuania

Received 03 February 2022; accepted 20 September 2022

Abstract. The paper investigates whether foam glass could reduce the structural thickness of the protection layer in the construction of the railway track (saving of natural materials – crushed aggregate) and, at the same time, also provide sufficient thermal protection of the frost-susceptible subgrade surface. It also discusses whether the incorporation of foam glass would have a relevant effect on the increase of the deformation resistance of the railway track structure at the level of the sub-ballast upper surface. Following these assumptions, the paper presents the results of experimental measurements of the deformation resistance of the modified structural composition of the sub-ballast layers (with an embedded foam glass layer) and their comparison with the results determined on a structure with a standard composition of the sub-ballast layers (crushed aggregate sub-ballast layer/protective layer). Also, numerical and mathematical analysis of the influence of the built-in thermal insulation foam glass layer on the reduction of the structural thickness of the protective crushed aggregate layer in terms of the effect of climatic factors is conducted in the paper. The mathematical model, developed by the research, provides the possibility of continuous monitoring of the change in the railway track structure freezing depending on climatic characteristics.

Keywords: railway track, sub-ballast layers, thermal insulation layers, foam glass, static load tests, climatic factors.

Introduction

Rail transport is also often referred to as green transport due to lower energy consumption, lower noise production and, last but not least, lower greenhouse gas production of rail transport compared to other transport systems. A 2018 EU analysis indicated that rail transport accounted for only 0.4% of the overall GHG transport emissions. This proportion is negligible compared to road transport that is ubiquitous and more burdensome to the environment, producing more than 71% emissions (Republic of Slovenia Statistical Office, 2018). The development and modernisation of the rail network are, therefore, one of the EU's priorities, with a strong emphasis on ensuring sustainable development and reusing material resources. One of the waste materials that deserve increased attention is glass due to its long decomposition time (estimated to 4000 years). At present, among other products, waste

glass is used for the production of foam glass, which, thanks to some of its distinctive properties, is constantly finding new applications, for example as a thermal insulation material. The objective of the present paper is thus to assess the possibility of applying foam glass as a secondary building material in the structural composition of the sub-ballast layers, with a specific focus on its excellent thermal insulation properties. In the case of sub-ballast layers of fine-grained soils, this means achieving its complete thermal protection, which, together with a possible increase in the deformation resistance of the sub-ballast layers, would create conditions for a long-term safe and stable roadway.

Ensuring long-term shape and volume stability and, at the same time, deformation-resistant construction of the sub-ballast layers can generally be achieved by selecting appropriate construction materials and thicknesses of its

*Corresponding author. E-mail: deividas.navikas@vilniustech.lt

structural layers. In addition to the transport load, the sub-ballast layers are also subjected to non-transport loads – the effect of weather and climatic factors. If the magnitude and thus the effect of the traffic load can be influenced, the effect of the non-traffic load on the railway track cannot be excluded and affects the quality of the railway track throughout the year, especially during the winter and spring seasons. In particular, the effect of frost on the sub-ballast layers is one of the main factors of non-traffic loads that significantly affects its quality, especially in relation to the unfavourable water regime and the frost-susceptible subgrade surface (Bąk & Chmielewski, 2019).

The effectiveness of the whole structure of the track substructure concerning the protection against the adverse effects of frost is expressed in terms of thermal resistance. The greater the thickness of the individual structural layers and/or the lower the thermal conductivity coefficients of the incorporated building materials, the higher the overall thermal resistance of the structure. Therefore, the incorporation of high-efficiency thermal insulation materials ($\lambda < 0.4 \text{ W}\cdot\text{m}^{-1}\cdot\text{K}^{-1}$) in the structural sub-ballast layers allows, from the point of view of its protection against freezing of the frost-susceptible subgrade surface, a reduction of the structural thickness of the protective subgrade surface layer of standard natural materials (crushed aggregate or gravel sand).

Currently, there are some high-performance thermal insulation materials with constantly evolving and expanding properties and applications on the construction market. The research of the Department of Railway Engineering and Track Management (DRETM) has long focused on monitoring the influence of traffic and non-transport (climatic) loads on the deformation resistance of the sub-ballast layers, as well as on the assessment of the possibilities of application of various thermal insulation materials in the structural sub-ballast layers (extruded polystyrene, liapor, liaporconcrete, composite foam concrete, foam glass). The research involved the construction of a 1:1 scale model of the railway line, consisting of 6 different structures of the sub-ballast layers (Ižvolt et al., 2021). Here, the thermal-technical parameters of the materials applied to the sub-ballast layers were determined (Ižvolt et al., 2013). The water regime of the subgrade surface of all 6 structures of sub-ballast layers was also monitored using the TDR method (Pieš & Můcová, 2019). Currently, the DRETM research focuses on monitoring the traffic load, its static (on the experimental stand) and dynamic (on real experimental sections of modernised lines) components.

Abroad, the application of thermal insulation materials in the sub-ballast layers was addressed, for example, in the Netherlands (Esveld & Markine, 2003), where expanded polystyrene (EPS) plates were applied in the structural composition of the sub-ballast layers (specifically on the subgrade surface) of a high-speed line (with a non-standard superstructure of the Rheda 2000 type). The EPS application in the structural composition of the sub-ballast layers indicated the most positive results in the case of

a low deformation-resistant subgrade (maintenance costs were significantly reduced). In research conducted in Finland (Nurmikolu & Kolisoja, 2005), extruded polystyrene boards (XPS) were applied in the sub-ballast layers, specifically at the level of the sub-ballast upper surface. The research results pointed out the necessity to tighten the compressive strength requirements of the boards for the case of high axle loads and to modify the design value of the thermal conductivity of the XPS thermal insulation boards to $0.050 \text{ W}\cdot\text{m}^{-1}\cdot\text{K}^{-1}$.

In turn, research implemented in the UK (Woodward et al., 2012) focused on the application of polyurethane boards in critical areas of railway tracks, namely transition areas to artificial structures (underpasses, culverts, bridges, tunnels). It confirmed the suitability of the application of polyurethane polymers called XiTRACK to stabilise and increase the stability of railway lines, especially in critical areas of increased dynamic effects of passing railway vehicles (e.g., switches, track crossings or transition areas). Another option for the application of thermal insulation materials, namely artificial aggregates (aggregates made from old recycled tyres – TDA or light expanded clays – LECA), in combination with standard aggregates (gravel) in the railway track embankment was considered in the USA research (Sadrihezahad et al., 2019). The results demonstrated that the application of TDA and LECA reduces the overall settlement and the rate of vibration propagation in the railway embankments, improving their stability and resistance to dynamic load or seismic effects. Artificial aggregate made of expanded clay – LECA or waste glass – GLASOPOR was also tested in the research implemented in Finland (Loranger et al., 2017). The output of their publication is the collected data necessary for the calibration of the numerical models. The use of another thermal insulation material, namely lightweight foam concrete, in the structural composition of transition zones for man-made structures was addressed in research conducted in China (Li et al., 2020). The research results indicated that the use of lightweight foam concrete in the structural composition of the transition area for artificial structures will provide reasonably satisfactory stability, and resistance even to large axial loads. Moreover, it will reduce the differential settlement of the bridge transition area, and distribute the stresses evenly to the subgrade of the railway track.

The content of the paper is related to the publication (Ižvolt et al., 2021), focused on the verification of the possibilities of application of extruded polystyrene in the sub-ballast layers and to the publications discussing the possibility of application of composite foam concrete in the structural sub-ballast layers (Ižvolt et al., 2019, 2022) or as a protective (sub-ballast) layer (Vlček & Valášková, 2021). The primary objective of the paper is to assess the possibility of applying foam glass aggregate fr. 0/63 mm to the structural sub-ballast layers in terms of the applied traffic load (its static component) and non-traffic (climatic) load.

The experimental measurements assessed the influence of the static component of the traffic load (static load tests) on the real modified construction of sub-ballast layers (built-in sub-ballast layer of foam glass and crushed aggregate) and standard construction of sub-ballast layers (only the sub-ballast crushed aggregate layer). The output of the experimental measurements are graphs enabling the design of the constructional composition of the standard or modified construction of sub-ballast layers in terms of the static component of the traffic load.

The numerical and mathematical analysis assessed the influence of the incorporation of a thermal insulation layer of foam glass aggregate fr. 0/63 mm on the reduction of the structural thickness of the protective crushed aggregate layer in terms of climatic factor effects (water and frost). Considering the experience of the subgrade surface freezing into the active zone in the direction from the track bench surface and from the embankment slope presented in Ižvolt et al. (2022), the numerical modelling of sub-ballast layers used a combination of two thermal insulation materials (foam glass aggregate and extruded polystyrene boards). The output of the numerical (mathematical) analysis is a design nomogram (mathematical relations) that enables to design the structural composition of the modified sub-ballast layers or the standard construction (structural layers) of the railway substructure. Application of foam glass aggregate in the sub-ballast layers is expected to reduce the protective layer (saving of natural materials – crushed aggregate, gravel sand) and effectively use waste glass.

1. Materials and methods

The subject of this chapter will be the characteristics of the modified structural composition of the sub-ballast layers (combination of a layer of granular foam glass material and a layer of crushed aggregate fr. 0/31.5 mm), the standard structural composition of the railway sub-ballast layers (consisting only of a crushed aggregate layer), the characteristics of the methodology for the determination of the deformation resistance of the tested structures and the numerical analysis conducted to assess the modified sub-ballast layers to the non-transport loads.

1.1. Foam glass

Foam glass is a porous glass foam material produced by heating a mixture of crushed or granulated glass and a chemical foaming agent. Limestone, calcium carbide or coke is used as the foaming agent. The mixture is roasted at a temperature of about 800 °C that releases gas from the foaming agent and creates a high number of closed and discontinuous pores in the glass (porosity of 80 to 90%, pore diameter of 0.1 to 5 mm). Foam glass is commercially available in the form of thermal insulation boards or as aggregates of different fractions. Since foam glass resists the rotting process and has completely closed pores, it can

be considered a highly suitable thermal insulation at the contact points with the frost-susceptible subgrade surface.

The first information on foam glass as a construction material was published by I. I. Kitaygorodskiy at the All-Union Conference on Standardization and Manufacture of New Construction Materials in Moscow as early as 1932 (Kitaygorodskiy, 1932). The product that is known today as cellular glass insulation Foamglas was developed by Pittsburgh Corning and was later acquired by Owens Corning. Thanks to some of its excellent properties (high thermal resistance, non-absorption, environmental friendliness), foam glass is continuously gaining popularity in building practice. Research on the properties of foam glass is being conducted abroad, e.g., in China, where it has so far been found that its mechanical properties are significantly influenced by the foaming agent (SiC). When the amount of foaming agent was reduced, the strength of the material increased (Bian et al., 2018). The thermal insulating properties of foam glass are also affected by the fly ash content, soda ash carbonate, as well as foaming temperature and time. Research results suggest that the more uniform and orderly the openings in the foam glass material are, the greater the thermal resistance of the material is, and thus the better its thermal insulation properties are (Qin et al., 2019). The structural, physical and mechanical properties of foam glass were also addressed in Malaysia (Hisham et al., 2021), where research demonstrated the effect of mixture composition and sintering temperature on the improvement of the foam glass properties in question. A correlation between the physical and thermal insulation properties of foam glass was established by Romanian research (Paunescu et al., 2021). It concluded that foam glass is a favourable alternative compared to known types of polymeric or fibreglass thermal insulation materials. The U.S. research indicated that the strength of foam glass is equally affected by different pore sizes (Morgan et al., 1981).

The basic technical and environmental properties of foam glass were also the subject of research in Australia (Arulrajah et al., 2015), where the health safety of this material was demonstrated. The concentrations of hazardous substances in the leachate were 100 times lower than drinking water standards. The dynamic resistance of foam glass and its impact on vibrations by railway traffic was addressed in Slovenia (Lenart & Kaynia, 2019). In this publication, numerical modelling of the use of foam glass aggregate embedded in a railway embankment was implemented. Due to all the above-mentioned properties and the obtained knowledge, the foam glass aggregate is also suitable for earthworks. Here it can be used as a lightweight fill material for embankments placed on poorly bearing soils and as a soil improvement material (Lu & Onitsuka, 2004). A study was also conducted on the possibility of applying foam glass as a thermal insulation material in pavement construction with foam glass as a suitable alternative for extruded polystyrene sheets (Ghafari et al., 2019; Frydenlund & Aaboe, 2003).

1.2. Properties of the applied materials – characteristics of the experimental field

One of the research activities currently being solved at DRETM is the assessment of the suitability of the application of thermal insulation materials in the sub-ballast layers, not only in terms of increasing their thermal resistance, but possibly also their deformation resistance at the level of the sub-ballast upper surface. For this reason, an experimental field (Figure 1), which enables to determine the deformation resistance of individual structural sub-ballast layers, was built on the premises of the University of Žilina. The experimental field is a part of the Experimental Stand DRETM (Ižvolt et al., 2021), built for the verification of the thermal-technical and deformation properties of the materials incorporated into the railway track structure.

Since the subject of the experimental measurements is the assessment of the influence of the built-in structural layer of foam glass aggregate on the increase of the deformation resistance of the sub-ballast layers, the experimental field consists of two segments. *Segment A* is a standard construction of sub-ballast layers (a sub-ballast crushed aggregate layer, fr. 0/31.5 mm) designed in the construction thickness according to the Slovak Technical Railway Standard (Directorate General of the Railways of the Slovak Republic, 2005). *Segment B* represents a modified construction of the sub-ballast layers – a combination of a sub-ballast layer of crushed aggregate fr. 0/31.5 mm and foam glass aggregate, fr. 0/63 mm. The subgrade of the sub-ballast layers at the level of subgrade surface of both segments can be characterised as not highly deformation resistant since in both cases the static modulus of deformation of the subgrade surface $E_0 = 10 \pm 2$ MPa was the baseline value. The Geofiltex 63/20 T separation geotextile was placed on the subgrade surface. As part of the modified construction of the sub-ballast layers (*Segment B*), a 150 mm thick layer of foam glass aggregate, fr. 0/63 mm was applied onto the subgrade surface. Subsequently, layers of crushed aggregate, fr. 0/31.5 mm gravel were placed on the surface of this thermal insulation layer, gradually reaching partial design thicknesses of 100, 200, 300 and 400 mm. The individual construction layers of crushed aggregate were compacted using a vibrating plate. Figure 1 demonstrates the ground plan and cross-section of the two segments of the experimental field and indicates the positions of the locations for determining the deformation resistance of the individual partial sub-ballast layers by static load tests. The basic physical and deformation characteristics of the construction materials incorporated in the experimental field structures are provided in Table 1.

textile was placed on the subgrade surface. As part of the modified construction of the sub-ballast layers (*Segment B*), a 150 mm thick layer of foam glass aggregate, fr. 0/63 mm was applied onto the subgrade surface. Subsequently, layers of crushed aggregate, fr. 0/31.5 mm gravel were placed on the surface of this thermal insulation layer, gradually reaching partial design thicknesses of 100, 200, 300 and 400 mm. The individual construction layers of crushed aggregate were compacted using a vibrating plate. Figure 1 demonstrates the ground plan and cross-section of the two segments of the experimental field and indicates the positions of the locations for determining the deformation resistance of the individual partial sub-ballast layers by static load tests. The basic physical and deformation characteristics of the construction materials incorporated in the experimental field structures are provided in Table 1.

1.3. Methodology for determining the deformation resistance of sub-ballast layers – Experimental Measurement

The experimental measurement of the deformation resistance of the standard (*Segment A*) and modified (*Segment B*) compositions of the sub-ballast layers of the experimental field was implemented using a static load setup and is demonstrated in Figure 2.

The experimental measurements followed the methodology presented in Directorate General of Railways of the Slovak Republic (2018), where a value of 0.20 MPa was used as the maximum value of the contact stress for both loading cycles of the static load test. The static load tests were performed in two loading cycles in which a rigid circular plate of 300 mm diameter was successively pushed into the surface of the tested structural sub-ballast.

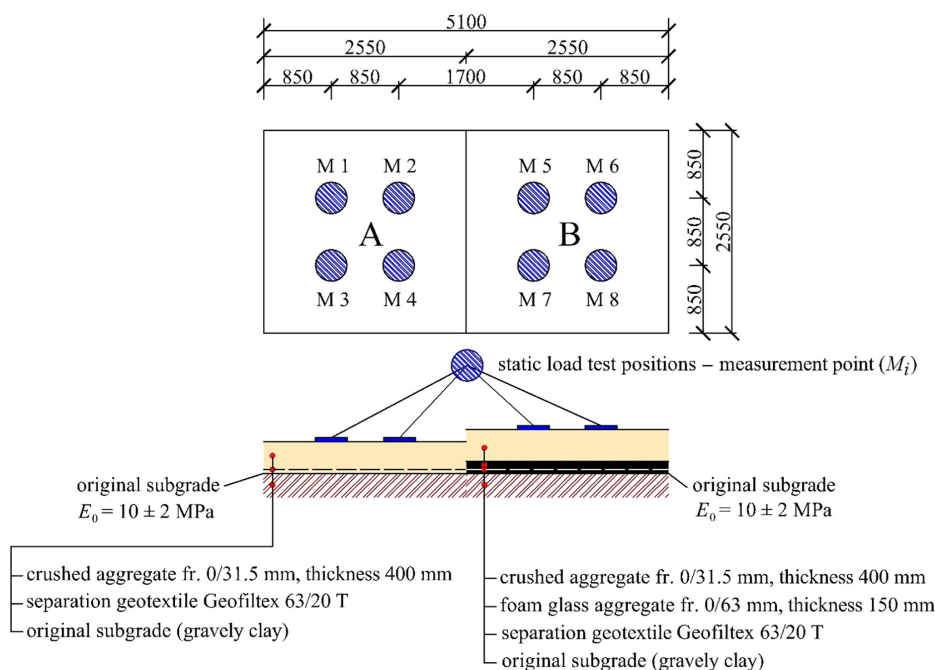


Figure 1. Experimental field: *Segment A* (standard sub-ballast layers), *Segment B* (modified sub-ballast layers)

Table 1. Physical and strength parameters of the applied materials

Material	Bulk density – dry (kg.m ⁻³)	Moisture (%)	Poisson's ratio (–)	Compressive strength (MPa)	Tensile strength (kN.m ⁻¹)
Crushed aggregate fr. 0/31.5 mm	1930	5.5	0.20	–	–
Foam glass fr. 0/63 mm	135 ± 10%	6	0.25	min. 0.17	–
Separation geotextile Geofiltex 63/20 T	200 ± 20 ¹	–	–	–	5.0
Subgrade – gravelly clay	1650	26	0.40	?	–

Note: ¹area weight 200 ± 20 g.m⁻² according to EN ISO 9864.



Figure 2. Implementation of static load test on the surface of foam glass aggregate

The resultant parameter is the static modulus of deformation E_{si} , obtained in the second loading cycle. The value of the static modulus of deformation E_{si} was calculated from the relation:

$$E_{si} = \frac{1.5 \cdot p \cdot r}{y}, \quad (1)$$

where E_{si} – static modulus of deformation of the i -th structural layer, (MPa); p – specific pressure acting on the plate, (MPa); r – radius of the load plate, (m); y – total average load-plate compression found in the second cycle, (m).

Since the static load tests were performed in two loading cycles, in addition to the deformation resistance on the surface of the partial structural sub-ballast layers, it was also possible to determine the quality of compaction of the embedded materials according to the methodology presented in Slovak Office of Standards, Metrology and Testing (2017). The quality (degree) of compaction was determined by the ratio of static deformation moduli determined in the second and first loading cycles. The static modulus of deformation on the surface of each structural layer of the sub-ballast layers was always determined on the second day after the compaction of the structural layer in question. A series of 4 measurements were performed

on the surface of each structural layer of both segments (see Figure 1), with the static load tests always performed at the same location, indicated as measurement point M_i (*Segment A* – measurement points M_1 to M_4 and *Segment B* – measurement points M_5 to M_8). Specifically, the experimental measurement of the static modulus of deformation was performed at the level of the subgrade surface, on the surface of the foam glass aggregate and at the level of each crushed aggregate layer of structural thickness 100, 200, 300 and 400 mm.

1.4. Methodology for determining the freezing of sub-ballast layers – Numerical analysis

The numerical analysis of the modified structure of the sub-ballast layers (with built-in thermal insulation layer of foam glass) was conducted to assess the freezing of this structure and to determine the required dimensions of the individual sub-ballast layers depending on different climatic loads (air freezing index I_F and the average annual air temperature θ_m). The numerical models of the modified design of the sub-ballast layers were developed based on the experience presented in Ižvolt et al. (2021, 2022) using the SVHeat programme (Thode, 2012). These models feature 2D transition models of a double-track railway line (as the most common case) with an embankment height of 2.0 m.

The initial design of the numerical model includes 4 material construction layers (ballast bed thickness 500 mm, protective crushed aggregate layer of variable thickness – from 50 to 600 mm, 150 mm thick thermal insulation layer of foam glass and clay subgrade), marked in the model as regions (Figure 3 left). Later, based on the results of the numerical analysis, a fifth material area will be added, namely extruded polystyrene boards (protection of the subgrade surface from freezing into the active zone in the direction from the surface of the track bench and the embankment slope).

The material characteristics of the individual structural layers in the numerical model are provided in Table 1 (see Section 1.2). Their thermal-technical characteristics were specified based on laboratory measurements (ballast bed, crushed aggregate, clay) (Ižvolt et al., 2013), technical data sheets declared by the manufacturer (thermal insulation materials) or experience from abroad papers (Glapor, n.d.; Gnip et al., 2001; Styrodur, 2019), and are presented in Table 2.

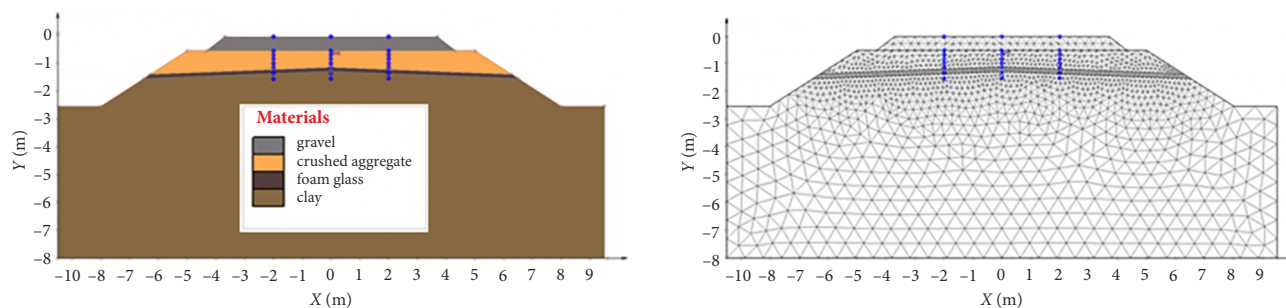


Figure 3. Numerical model (initial design) and use of FlexPDE in the analysis

Table 2. Thermal-technical parameters of the materials of the numerical model

Construction layer/ material characteristics	Ballast bed (moderate pollution)	Protective layer	Thermal insulation layer	Thermal insulation layer	Subsoil
Material of the layer	gravel fr. 31.5/63 mm	crushed aggregate fr. 0/31.5 mm	foam glass fr. 0/63 mm	extruded polystyrene boards	clay
Temperature (°C)	-2	3	4	-2	10
Specific heat capacity (J·kg ⁻¹ ·K ⁻¹)	980	1090	850	2060	1095
Thermal conductivity coefficient (W·m ⁻¹ ·K ⁻¹)	1.0	1.73	0.12	0.04	1.55

In the individual numerical models, the climatic stress was defined at the edges of the material regions in contact with the air. The main parameter for the climatic load was the mean daily air temperature θ_s defined for the whole analysed period. The mean daily air temperatures were entered in such a way that for the numerical model loaded with the most severe climate load, they characterised the air freezing index $I_F = 1400$ °C, day, and the average annual air temperature $\theta_m = 2$ °C (Figure 4). The air freezing index $I_F = 1400$ °C, day considers the threshold where a greater design thickness of the foam glass layer would be needed in the active zone of the sub-ballast layers, or where it would be appropriate to use another thermal insulation material with more suitable thermal-technical parameters (e.g., polyurethane boards, extruded polystyrene boards, etc.) in combination with a sufficient thickness of the protective crushed aggregate layer (to ensure sufficient deformation resistance of the structure at the level of the sub-ballast upper surface).

In the other numerical models, the climatic load was progressively reduced by using air freezing index values of $I_F = 1300, 1200, 1100$ and 1000 °C, day, and corresponding average annual air temperature values of $\theta_m = 2, 3$ and 4 °C. The lower limit of the climatic load, namely the air freezing index $I_F = 1000$ °C, day and the average annual air temperature $\theta_m = 4$ °C, were determined on the basis that for the specific climatic load a design of a smaller thickness of the protective layer of crushed aggregate than the minimum required technological thickness (150 mm) was necessary. The climatic characteristics were determined due to measured values of mean daily air temperatures θ_s obtained from various meteorological stations located in the territory of Slovakia.

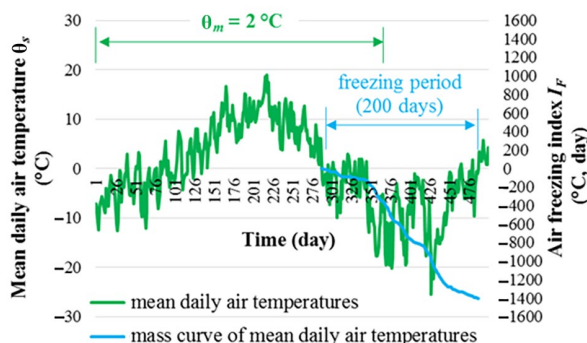


Figure 4. Maximum climate stress used in the numerical modelling (air freezing index $I_F = 1400$ °C, day and average annual air temperature $\theta_m = 2$ °C)

The average annual air temperature θ_m in the numerical models defines the range of days TIME = 1 to TIME = 365. The freezing period in the numerical model is defined for an air freezing index of $I_F = 1400$ °C, day and average annual air temperature $\theta_m = 2$ °C over a period of 200 days (from 15 October to 2 May - TIME = 289 to TIME = 488). As the climatic load decreased, a shorter freezing period was defined, with a length of 180 days for the lower limit of the climatic load ($I_F = 1000$ °C, day). The numerical models also consider the influence of snow cover expressed by the nf factor (factor expressing the dependence between the mean daily air temperature and the temperature on the ballast bed surface). In the numerical models, a value of $nf = 0.6$ (the value attributable to the thickness of the snow cover aligned to the top surface of the ballast bed) was used during the winter period. The influence of snow cover thickness on the nf factor values was presented in Ižvolt et al. (2018).

The calculation of the freezing of the structural layers of the railway track in numerical models was performed using the FlexPDE programme and the ACU-MESH programme was used to visualize the solution results (Fredlund & Haihua, 2011). The complex differential equations were solved using the infinite element method with a specified solution time step of 0.1 per day. The grid generation module constructs a triangular (3, 6, or 9-node triangles) finite element mesh over an arbitrary two-dimensional model domain (Figure 3, right). The mesh generator allows a spatially varying density of nodes in order to focus on areas of structural detail.

2. Results and discussion

The sub-ballast layers must have the ability to accept transport and non-transport (climatic) loads without harmful deformations in the long term. They can only have these properties if they are built of high-quality construction materials of the required structural thicknesses – dimensions. In this part of the paper, the results of experimental and numerical analyses focused on the design of a modified structural composition of the sub-ballast layers (with a built-in thermal insulation layer of foam glass aggregate fr. 0/63 mm) will be characterised in terms of the static component of the traffic load as well as the effect of non-traffic load.

2.1. Deformation resistance of the sub-ballast layers

The determination of the deformation resistance on the surface of the partial structural layers of the sub-ballast layers was performed on the experimental field using the methodology described in more detail in Section 1.3. The characteristics of the individual segments, material and structural composition of the experimental field were specified in Section 1.2. The measured values of the deformation resistance (static modulus of deformation E_{si} on the surface of the partial structural layers representing the standard structural composition of the sub-ballast layers (*Segment A*) are demonstrated in Figure 5.

The values of the static modulus of deformation E_{si} , specified in Figure 5, will be compared with the values identified for the modified structural layer composition of the sub-ballast layers (*Segment B*), Figure 6.

The comparison of the results specified in Figure 5 and Figure 6 indicates that as the design thickness of the crushed aggregate layer increases, the equivalent value of the modulus of deformation also increases. This finding is valid for larger structural thicknesses of the crushed aggregate layer – from approx. 300 mm onwards, when the measured value of E_{si} is no longer affected by the small deformation resistance of the subgrade surface ($E_0 = 10 \pm 2$ MPa). The measured values at the level of the sub-ballast upper surface (in this case on the surface of the 400 mm thick crushed aggregate layer) indicate a higher value of the static modulus of deformation of the modified design of the sub-ballast layers (150 mm thick layer of foam glass

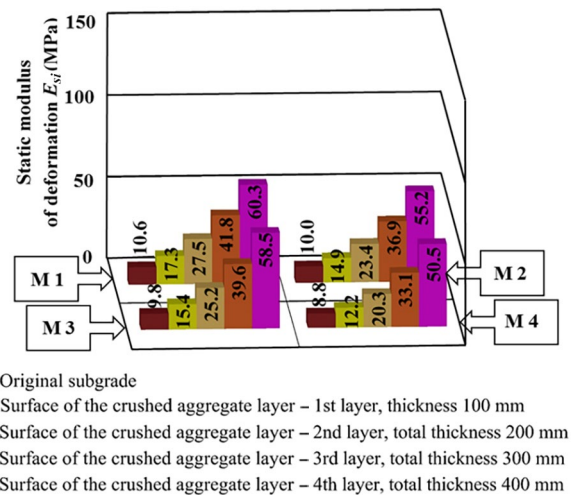


Figure 5. Values of the static modulus of deformation E_{si} measured on the surface of the partial layers of the standard structural composition of the sub-ballast layers (*Segment A*)

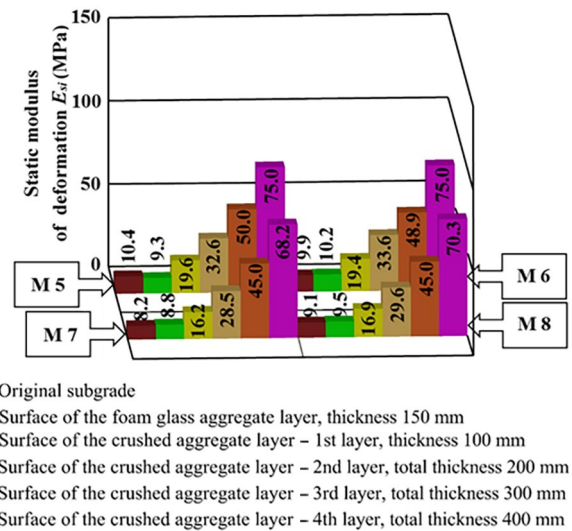


Figure 6. Values of the static modulus of deformation E_{si} measured on the surface of the partial layers of the modified structural composition of the sub-ballast layers (*Segment B*)

aggregate + 400 mm thick layer of crushed aggregate) by approx. 12 to 20 MPa compared to the standard design of the sub-ballast layers (only 400 mm thick layer of crushed aggregate). The experimental measurements also determined the degree of compaction of the measured structural layer in question, with comparable values achieved in both the *Segment A* and *Segment B* designs. For the 1st and 2nd construction layer of crushed aggregate, a compaction rate (quality) of 1.70 to 1.90 was achieved, and for the case of the 3rd and 4th construction layer of crushed aggregate (level of the sub-ballast upper surface), a compaction rate of 1.50 to 1.65 was achieved. Since the minimum allowable compaction rate for coarse-grained materials according to Slovak Office of Standards, Metrology and Testing (2017) is 2.60, the measured values of the compaction rate were satisfactory in all cases.

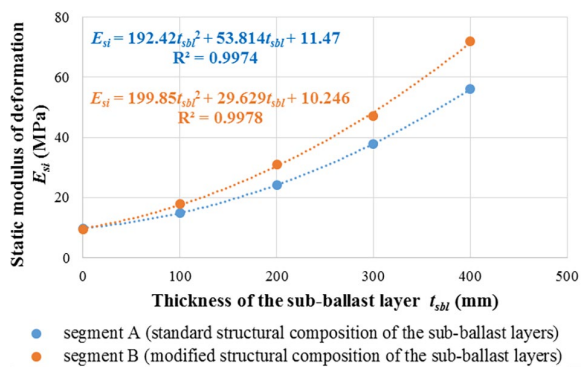


Figure 7. Comparison of standard (*Segment A* – crushed aggregate only) and modified (*Segment B* – crushed aggregate + 150 mm of foam glass aggregate) structural composition of the sub-ballast layers

Figure 7 demonstrates a comparison of the standard (*Segment A*) and modified (*Segment B*) structural composition of the sub-ballast layers, where the values of the static deformation moduli E_{si} are presented as average values for each structural layer (average values of the static deformation moduli E_{si} from 4 measurements on the surface of each structural layer).

Figure 7 indicates that the difference in the deformation resistance of the standard and modified sub-ballast layers increases with the increasing thickness of the sub-ballast layer t_{sbl} of crushed aggregate. This means that the 0/63 mm layer of foam glass aggregate in the present design has a certain influence on the increase of the overall deformation resistance of the structural sub-ballast layers. This claim is predictable due to the structural thickness of the protective subgrade surface which is larger than in the case of the modified sub-ballast layers design.

However, if the same design thickness of the sub-ballast layer (protective layer) of the standard and modified designs of the sub-ballast layers is compared, in the case of the standard design of the sub-ballast layers, it is a 400 mm thick sub-ballast layer of crushed aggregate and in the case of the modified design, it is a 150 mm thick design layer of foam glass aggregate and a 250 mm thick design layer of crushed aggregate. In this way, more relevant insight into the actual effectiveness of the foam glass aggregate on the overall deformation resistance of the structure can be obtained.

The comparison of the structural composition of the sub-ballast layers (the structural thickness of the protection subgrade surface layer) indicates that the standard structural composition of the sub-ballast layers is more deformation-resistant (E_{si} of about 56 MPa) than its modified structural composition (E_{si} of about 40 MPa). The 0/63 mm foam glass aggregate layer does not contribute to increasing the overall deformation resistance of the sub-ballast layers at the level of the subgrade surface, but, as demonstrated below, only has an excellent thermal insulation effect, i.e. it protects the frost-susceptible subgrade surface from freezing.

This finding implies that if a higher value of deformation resistance is to be achieved at the level of the sub-bal-

last upper surface, a higher design thickness of crushed aggregate must be considered, since the structural layer of foam glass has a significantly lower value of deformation resistance than an equally thick structural layer of crushed aggregate. By incorporating a 150 mm thick structural layer of foam glass aggregate fr. 0/63 mm, it is generally possible to reduce an approx. 50 mm thick layer of 0/31.5 mm crushed aggregate.

The experimental measurement results of deformation resistance demonstrated in Figure 7 indicate that for the case of deformation resistance of subgrade surface of $E_0 = 10 \pm 2$ MPa, a deformation resistance value of E_{si} of about 20 MPa was obtained on the surface of the 150 mm thick crushed aggregate structural layer, and a deformation resistance value of E_{si} of only about 10 MPa was obtained on the surface of the 150 mm thick foam glass structural layer. This means that the 150 mm thick foam glass structural layer material had no effect on the increase of the deformation resistance under these boundary conditions, or the crushed aggregate material will cause an increase of the deformation resistance of the structure compared to the foam glass material by 100% in this case (low deformation resistant subgrade surface).

2.2. Resistance of the modified structure to non-traffic loads – design nomogram

The aim of the numerical analysis was to create a numerical model of the sub-ballast layers that will be sufficiently resistant to the defined climatic loads specified in more detail in Section 1.4, and thus the frost-susceptible subgrade surface will not freeze in the entire active zone of the traffic load. A comparison of the real structure with the numerical model, in order to verify the relevance of the numerical modelling input data, has been elaborated in previous papers (Ižvolt et al., 2020, 2021, 2022). In the first step, a numerical model of the railway track in embankment (Figure 8) was developed. It included the design of a foam glass thermal insulation layer of structural thickness 150 mm over the entire width of the subgrade surface, combined with a crushed aggregate layer of structural thickness of 600 mm. The thickness of the crushed aggregate layer was designed depending on the applied climatic load for freezing index $I_F = 1400$ °C, day and average annual air temperature $\theta_m = 2$ °C (maximum climatic load considered in the numerical analysis) according to the legislative document (Directorate General of the Railways of the Slovak Republic, 2005). These design layer thicknesses were proposed because the protective layer of crushed aggregate, of design thicknesses of 250 mm and 400 mm (as proposed by assessing the design thickness of the sub-ballast layer for the static loads resulting from Section 1.2 and Section 2.1 respectively), are insufficient in terms of non-traffic loads.

Figure 8 (right) depicts the maximum depth of freezing achieved in numerical model 1, represented by the zero isotherm (red curve). The course of the zero isotherm demonstrates that the design of the sub-ballast layers in

numerical model 1 prevented the embankment subgrade surface from freezing in the track centreline region. However, the freezing already occurs before the end of the active zone of the traffic load effects (the active zone is considered about 2.50 m from the track centreline). In order to ensure the protection of the embankment subgrade surface against freezing in the direction from the embankment slope and from the track bench surface, a numerical model 2 was defined (Figure 9). The numerical model No. 2 differs from the previous model by a thicker thermal insulation layer of foam glass aggregate (design thickness 250 mm) in the area of contact with the embankment slope (to a width of 2.50 m from the embankment slope).

Figure 9 (right) demonstrates that numerical model 2 is suitable with respect to the protection of the subgrade

surface from freezing over the entire width of the active zone of the traffic load effects, but requires the incorporation of a larger amount of foam glass aggregate.

For that reason, and based on the experience gained from the numerical analysis implemented in İzvolt et al., (2022), numerical model No. 3 was developed (Figure 10). Numerical model No. 3 is characterised by the replacement of a part of the foam glass material in the area where the increased freezing of the subgrade surface of the sub-ballast layers in the embankment occurs, specifically in the direction from its slope and from the surface of the track bench, with a thermal insulation material of better thermal insulation properties (boards of extruded polystyrene – XPS). Extruded polystyrene boards of 0.10 m thickness were designed for a width of 2.50 m from the contact of the subgrade surface of the embankment and

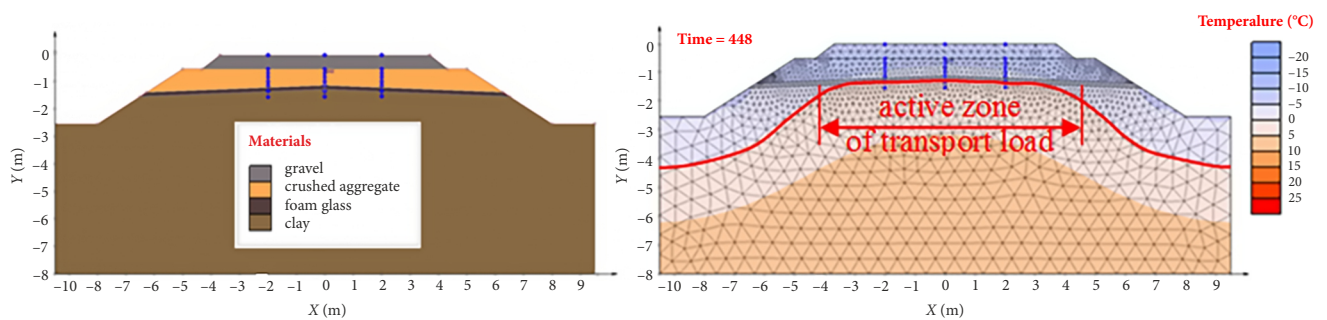


Figure 8. Numerical model No. 1: design of the body of the sub-ballast layers with built-in thermal insulation layer made of foam glass for the whole width of the embankment subgrade surface with respect to the applied climatic load $I_F = 1400 \text{ }^\circ\text{C}$, day and $\theta_m = 2 \text{ }^\circ\text{C}$ (left); the day of reaching the maximum freezing depth of the structural layers of the numerical model (right)

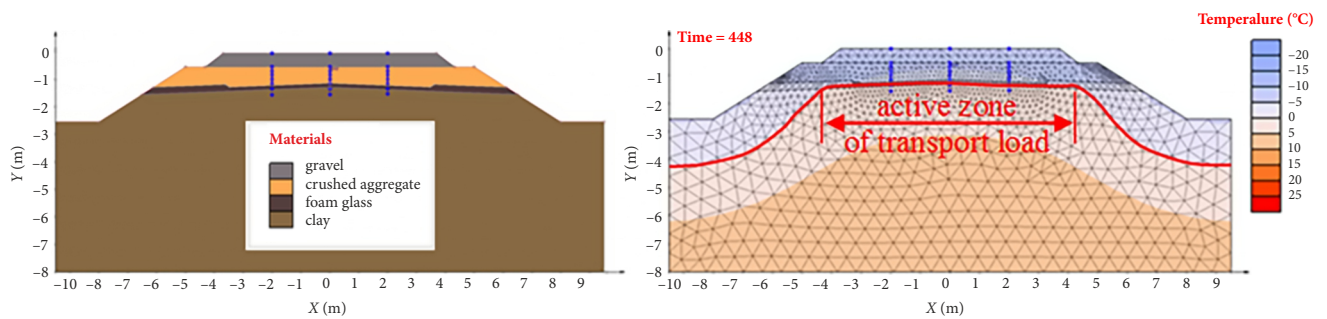


Figure 9. Numerical model 2: design of different thicknesses of the foam glass layer in the sub-ballast layers with respect to the applied climatic load $I_F = 1400 \text{ }^\circ\text{C}$, day and $\theta_m = 2 \text{ }^\circ\text{C}$ (left); day of achieving the maximum freezing depth of the structural layers of the numerical model (right)

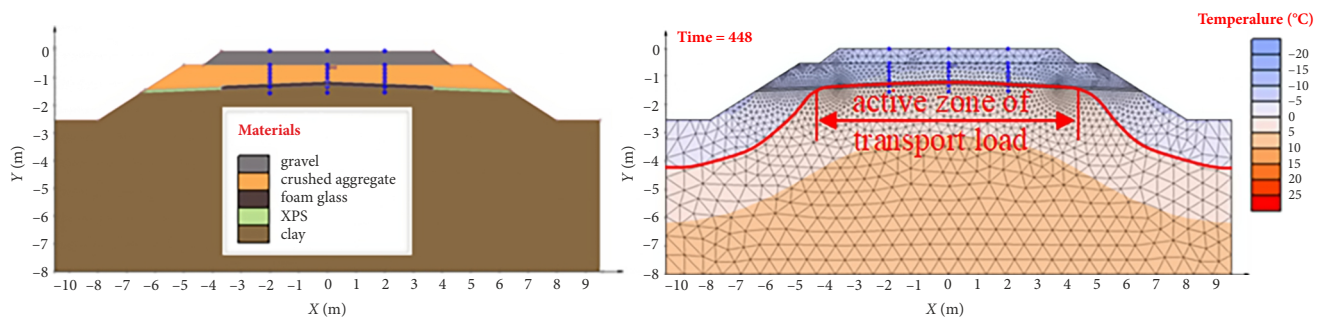


Figure 10. Numerical model 3: design of the combination of two thermal insulation materials (foam glass and extruded polystyrene) in the sub-ballast layers with respect to the applied climatic load $I_F = 1400 \text{ }^\circ\text{C}$, day and $\theta_m = 2 \text{ }^\circ\text{C}$ (left); day of achieving the maximum freezing depth of the structural layers of the numerical model (right)

its slope.

Figure 10 (right) demonstrates that the numerical model 3 is suitable in terms of protecting the embankment subgrade surface against freezing over the entire width of the active zone of the traffic load effects, in the case of the maximum climatic load considered in the numerical analysis ($I_F = 1400$ °C, day and $\theta_m = 2$ °C). For this reason, the structural composition of the sub-ballast layers of the numerical model 3 was also subsequently used to create the design dimensioning nomogram (Figure 11). The design nomogram is to be used for the final design of the necessary design thickness of the crushed aggregate layer, which in combination with the thermal insulation materials (foam glass aggregate fr. 0/63 mm of 150 mm design thickness and XPS boards of 100 mm design thickness – see Figure 10 left), will provide the required protection of the frost-susceptible subgrade surface against freezing, depending on the different climatic loads (freezing index I_F and average annual air temperature θ_m). The thickness of the structural crushed aggregate layer in the individual numerical models was progressively adjusted depending on the different climatic loads, in such a way that the final structural layer composition in the model would resist freezing of the frost-sensitive subgrade surface in the active zone of the traffic load effects.

The range of climatic loads used in the development of the design nomogram is further specified in Section 1.4. In addition, the design nomogram is supplemented with curves to allow the design of the necessary thickness of the crushed aggregate layer for the case of a standard sub-ballast layers design (without the application of thermal insulation materials in the sub-ballast layers design), depending on the different climatic loads (Ižvolt et al., 2022). Thanks to this measure, it is also possible to compare the standard and modified design of the sub-ballast layers and to determine the possible saving of natural materials (crushed aggregate).

Figure 11 demonstrates that in the case of a modified design of the sub-ballast layers, and in terms of non-traffic loads for areas with an air freezing index of, e.g., $I_F = 1200$ °C, day and an average annual air temperature of $\theta_m = 3$ °C, it would be necessary to design a construction layer of crushed aggregate with a thickness of $t_{pl} = 350$ mm, in combination with foam glass aggregate layer with a construction thickness of 150 mm and extruded polystyrene (XPS) boards with a thickness of 100 mm. The construction arrangement as depicted in Figure 10.

In the case of the standard design of the sub-ballast layers, it would be necessary to design a crushed aggregate layer of 1100 mm design thickness. However, in the case of the standard design of the sub-ballast layers, the entire active zone of the traffic load would not be protected from freezing. Freezing would occur in the direction from the embankment slope and from the surface of the track bench.

The modified structural composition of the sub-ballast layers needs to be assessed in terms of the application of

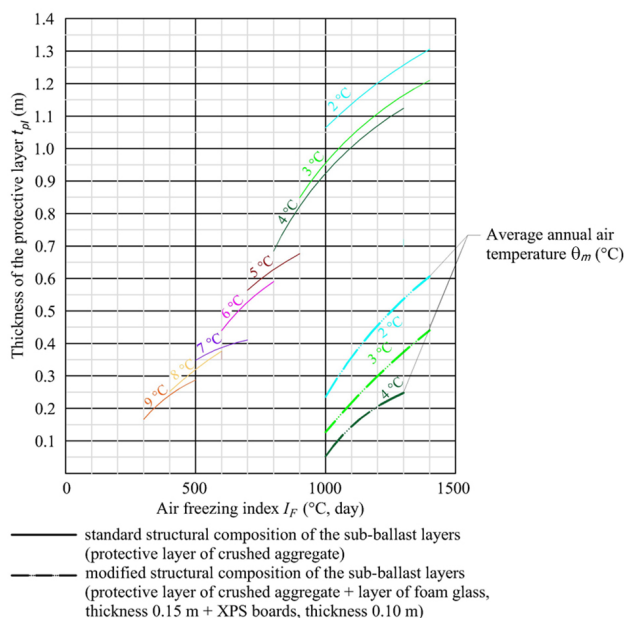


Figure 11. Design nomogram: dependence of the thickness of the crushed aggregate protection layer on different climatic conditions for standard and modified construction of the sub-ballast layers

the traffic load (see Section 2.1). The freezing indices $I_F < 1000$ °C, day were not interpreted in the numerical analysis of the modified structural composition of the sub-ballast layers, since for the given climatic load the design of a minimum thickness of the structural layer of 150 mm of crushed aggregate, in combination with foam glass aggregate, would be sufficient. The design of XPS boards would not be necessary.

The numerical analysis also produced numerical models with the thickness of the foam glass aggregate layer increased to 200 mm. In the case of these models, increasing the thickness of the foam glass aggregate layer by 50 mm allows reducing the design thickness of the crushed aggregate layer by an additional 150 mm, compared to the thickness determined according to Figure 11 (in the case of dimensioning the modified design depending on the climatic load). In many cases, a subsequent increase in the thickness of the crushed aggregate structural layer would be necessary, e.g., in the case of the assessment of the structural sub-ballast layers for deformation resistance as the benefit of the increased structural thickness of the foam aggregate layer is negligible.

2.3. Design of the modified structure of the sub-ballast layers in respect to non-traffic load – mathematical model

From the numerical modelling of the obtained data (Section 2.2) and from the design nomogram for dimensioning the sub-ballast layers for non-traffic loads – Figure 11, it was possible to create a continuous mathematical model to monitor the influence of the incorporated thermal insulation layer of foam glass aggregate on the reduction

of the thickness of the protective crushed aggregate layer. The design considers the effects of climatic factors that are the air freezing index I_F and the average annual air temperature θ_m .

Based on the distribution of numerically obtained data and the discrete dependence of the depth of freezing of the railway track structure D_F on the value of the air freezing index I_F and the average annual air temperature θ_m , the influence of the embedded thermal insulation layer in the form of foam glass aggregate can be approximated partially by a power function:

$$D_F = c\theta_m^a I_F^b, \text{ where } \theta_m > 0, I_F > 0. \quad (2)$$

This function was based on the knowledge and dependencies already established for extruded polystyrene (Ižvolt et al., 2021) and foam concrete (Ižvolt et al., 2022). Using a sufficiently stable least squares method (Buša et al., 2006), when the sum of squared deviations between the obtained and approximated data is to be minimal, the unknown coefficients a, b, c must be determined in the search for the minimum of the sum function:

$$S(a, b, c) = \sum_{i=1}^n (c\theta_{mi}^a I_{Fi}^b - D_{Fi})^2. \quad (3)$$

Using the linearization of the problem, the least squares method and the procedure given in (Ižvolt et al., 2021), after denoting $C = \ln c$, $x_i = \ln \theta_{mi}$, $y_i = \ln I_{Fi}$, $f_i = \ln D_{fi}$, $i = 1, \dots, n$ we obtain a system of equations:

$$C = \left(\sum_{i=1}^n f_i - a \sum_{i=1}^n x_i - b \sum_{i=1}^n y_i \right) / n, \\ aQ_{xy} + bR_y - Q_{fy} = 0, aR_x + bQ_{xy} - Q_{fx} = 0, \quad (4)$$

where: $Q_{uv} = \left(n \sum_{i=1}^n u_i v_i - \sum_{i=1}^n u_i \sum_{i=1}^n v_i \right) / n,$

$$R_u = n \sum_{i=1}^n u_i^2 - \left(\sum_{i=1}^n u_i \right)^2.$$

The solutions of the system of linear Eqns (4) are:

$$a = (Q_{fy}Q_{xy} - R_yQ_{fx}) / (Q_{xy}^2 - R_xR_y), \\ b = (Q_{fx}Q_{xy} - R_xQ_{fy}) / (Q_{xy}^2 - R_xR_y), \quad c = e^C. \quad (5)$$

The global error of this approximation is determined by the relation:

$$\varepsilon = \sqrt{\sum_{i=1}^n (c\theta_{mi}^a I_{Fi}^b - D_{Fi})^2} / n. \quad (6)$$

At a freezing index value of $I_F = 900$ °C, day there is a change in the properties that were comprehensively entered into the numerical model and that also affect the depth of freezing of the railway structure. Therefore, all these influences have to be considered. Also, the approximation function sought for the continuous monitoring of the freezing depth of the railway track without the use of a thermal insulation layer in the sub-ballast layers will

vary in this value and has a different expression for the case of the protective subgrade surface layer of crushed aggregate only.

In the case of climatic conditions for $I_F \leq 900$ °C, day and $\theta_m \geq 2$ °C and the construction of the protective subgrade surface layer of crushed aggregate, without the use of a thermal insulation layer in the sub-ballast layers, the following relations apply for the calculation of the depth of freezing of the railway track structure, or the necessary thickness of the protective layer:

$$D_F = 0.1436\theta_m^{-0.28} I_F^{0.374}; \quad (7)$$

$$t_{PL} = D_F - 0.5 = 0.1436\theta_m^{-0.28} I_F^{0.374} - 0.5, \quad (8)$$

where $I_F \leq 900$ °C, day.

Considering all the complex properties of the railway track structure, the mathematical model is for $I_F > 900$ °C, day and $\theta_m \geq 2$ °C:

$$D_F = 0.2808\theta_m^{-0.33} I_F^{0.3}; \quad (9)$$

$$t_{PL} = D_F - 0.5 = 0.2808\theta_m^{-0.33} I_F^{0.3} - 0.5, \quad (10)$$

where $I_F > 900$ °C, day. The global error for both these mathematical models is $\varepsilon \doteq 0.0117$.

According to the above procedure, in the case of unfavourable climatic conditions ($I_F \geq 900$ °C, day and $\theta_m < 5$ °C) and the reduction of part of the protective crushed aggregate layer by thermal insulation material – foam glass aggregate of thickness $z_i = 150$ mm, the approximation functions depending on the air freezing index I_F and the average annual air temperature θ_m for the calculation of the depth of freezing D_F of the railway track structure and the required thickness of the protective layer t_{PL} are expressed as follows:

$$D_F = 0.00121\theta_m^{-0.34} I_F^{0.99}; \quad (11)$$

$$t_{PL} = D_F - 0.65 = 0.00121\theta_m^{-0.34} I_F^{0.99} - 0.65, \quad (12)$$

where $I_F \geq 900$ °C, day.

The global error for the determined approximation functions is $\varepsilon = 0.014$. The deviations ΔD_F between the data obtained by mathematical and numerical modelling are in the interval $-0.02; 0.01$.

Table 3 demonstrates the difference $\Delta D_F = D_{F, mat} - D_{F, num}$ between the data calculated by the mathematical model (Eqns (7), (9), (11)) and the data obtained by the numerical modelling presented in Section 2.2. The values obtained by the mathematical model are rounded to two decimal places. Subsequently, when rounded up to a number divisible by five, the same values as for the numerically obtained data are acquired and, for practical purposes, rounded up to a multiple of 50 mm. The mathematical model thus characterises the depth of freezing of the railway line as well as the necessary thickness of the protective layer of the subgrade surface of the railway line structure in a sufficiently accurate and continuous manner.

Table 3. Deviations of the values determined by mathematical and numerical methods for the depth of freezing of the railway track structure D_F as a function of the air freezing index I_F and the average annual air temperature θ_m (sub-ballast layers without thermal insulation layer and with built-in thermal insulation layer made of foam glass of 150 mm thickness)

Without thermal insulation layer $z_i = 0$ mm					With thermal insulation layer $z_i = 150$ mm				
I_F (°C, day)	θ_m (°C)	$D_{F, mat.}$ (m)	$D_{F, num.}$ (m)	ΔD_F (m)	I_F (°C, day)	θ_m (°C)	$D_{F, mat.}$ (m)	$D_{F, num.}$ (m)	ΔD_F (m)
1000	2.0	1.560	1.564	0.002	1000	2.0	0.890	0.900	-0.010
1100	2.0	1.620	1.642	-0.022	1100	2.0	0.980	1.000	-0.020
1200	2.0	1.690	1.196	-0.006	1200	2.0	1.070	1.090	-0.020
900	3.0	1.340	1.338	0.002	1300	2.0	1.160	1.160	0.000
1000	3.0	1.480	1.470	0.010	1400	2.0	1.240	1.250	-0.010
1100	3.0	1.550	1.542	0.008	900	3.0	0.700	0.700	0.000
1000	4.0	1.430	1.428	-0.015	1000	3.0	0.780	0.800	-0.020
700	5.0	1.060	1.064	-0.004	1100	3.0	0.860	0.860	0.000
800	5.0	1.110	1.129	-0.019	1200	3.0	0.930	0.940	-0.010
900	5.0	1.170	1.176	-0.006	1300	3.0	1.010	1.030	-0.020
600	6.0	0.950	0.944	0.006	1400	3.0	1.080	1.100	-0.020
700	6.0	1.010	1.026	-0.016	1000	4.0	0.700	0.700	0.000
500	7.0	0.850	0.849	0.001	1100	4.0	0.780	0.800	-0.020
400	8.0	0.750	0.752	-0.002	1200	4.0	0.840	0.850	-0.010
500	8.0	0.820	0.820	0.000	1300	4.0	0.920	0.910	0.010

The determined approximation functions for the calculation of the freezing depth of the railway track structure as a function of the average annual air temperature θ_m and the air freezing index I_F are sufficient, since the determined thickness is rounded up to the nearest 50 mm in the dimensioning of the thickness of the protective crushed aggregate layer. A global calculation error of up to 15 mm guarantees that the same resulting values are obtained after rounding the thickness of the crushed aggregate protection layer, even with the addition of the thermal insulation material, as after rounding the values obtained by numerical modelling.

Conclusions and future research

The DRETM research has long been focused on monitoring the different compositions of the sub-ballast layers from the point of view of the effects of non-traffic (climatic) loads (since 2003) and more recently also traffic (static) loads (since 2020). In addition to the standard construction materials, the research assesses the effects of various thermal insulation materials incorporated into the structural composition of the sub-ballast layers and investigates their influence not only on the increase of the thermal resistance of the structure, but also on the possible increase of its deformation resistance. In this context, the paper presents conducted experimental measurements and numerical analysis to assess the suitability of incorporating foam glass aggregate, fr. 0/63 mm, into the structural composition of the body of the sub-ballast layers to achieve savings of natural materials (crushed aggregate) and at the same time the use of recycled waste materials (in our case, glass). Based on these facts and results, it

can be concluded that: The incorporation of foam glass aggregate, fr. 0/63 mm and the thickness of 150 mm in the structural composition of the tested structure of *Segment B* (see Figure 1), has no significant effect on the increase of the overall deformation resistance of the sub-ballast layers at the level of the sub-ballast upper surface (see Section 2). However, as Figure 7 demonstrates, if an equally thick crushed aggregate structural layer is considered (400 mm structural thickness in both cases), then the difference between the deformation resistance of the standard (*Segment A*) and modified (*Segment B*) structural compositions of the sub-ballast layers increases with increasing thickness of the crushed aggregate structural layer. In this case of a 400 mm thick crushed aggregate layer, it is possible to achieve on average approximately 16 MPa more deformation resistance compared to the standard sub-ballast layers composition. The modified sub-ballast layers consist of a 150 mm thick structural layer of foam glass aggregate in addition to the 400 mm thick crushed aggregate layer). It should be noted, however, that the measured values were obtained for the case of a low deformation-resistant sub-grade surface ($E_0 = 10 \pm 2$ MPa):

1. By incorporating a 150 mm thick structural layer of 0/63 mm foam glass aggregate, it is generally possible to replace an approximately 50 mm thick layer of 0/31.5 mm crushed aggregate. The objective was to achieve the deformation resistance of 50 MPa at the level of the sub-ballast upper surface, which is the required value for the existing modernised lines under the administration of Slovak Railways classified in the speed zone SZ4, i.e. 120 to 160 km.h⁻¹) according to the legislative document (Directorate General of the Railways of the Slovak Republic,

- 2005). To achieve it, it would be necessary to design a structural layer of foam glass aggregate fr. 0/63 mm of 150 mm thickness and a 300 mm thick construction layer of crushed aggregate fr. 0/31.5 mm (modified construction of the sub-ballast layers). In the case of the standard construction, only a 350 mm thick layer of crushed aggregate fr. 0/31.5 mm would be required (see Figure 7). This finding demonstrates that the foam glass aggregate does not have an equivalent performance compared to the standard material (crushed aggregate) in terms of the assessment of the sub-ballast layers for deformation resistance. However, due to the superb thermal insulation properties of the foam glass material ($\lambda = 0.12 \text{ W.m}^{-1}.\text{K}^{-1}$) compared to crushed aggregate ($\lambda = 2.0 \text{ W.m}^{-1}.\text{K}^{-1}$), its use is assumed mainly due to the thermal protection of the subgrade surface.
2. The application of foam glass aggregate fr. 0/63 mm in the structural composition of the sub-ballast layers (modified construction) is assumed mainly for areas with climatic load $I_F > 800 \text{ }^\circ\text{C, day}$ (necessary design of a large thickness of the structural layer of crushed aggregate $t_{pl} > 600 \text{ mm}$ in the case of the standard construction – see Figure 11). As the climatic load increases, a more significant saving of natural material (crushed aggregate) can be achieved. For example, for an air freezing index of $I_F = 1200 \text{ }^\circ\text{C, day}$ and an average annual air temperature of $\theta_m = 3 \text{ }^\circ\text{C}$, it is possible to reduce the structural thickness of the crushed aggregate protection layer by up to 750 mm in the track centreline and replace it with foam glass aggregate in a structural layer thickness of only 150 mm (see Figure 11). Such a composition and dimensioning of the sub-ballast layers is usually also satisfactory in relation to the traffic load.
 3. For areas with the air freezing index $I_F < 1000 \text{ }^\circ\text{C, day}$, the design of the minimum required thickness of the protective crushed aggregate layer $t_{pl} = 150 \text{ mm}$, in combination with a thermal insulation foam glass layer with a design thickness of 150 mm, is sufficient to protect the frost-susceptible subgrade surface from freezing. In the case of areas with the air freezing index $I_F > 1000 \text{ }^\circ\text{C, day}$, the design of a greater thickness of the protective crushed aggregate layer in combination with a 150 mm thick foam glass layer is required (see Figure 11). In addition, it is necessary to secure the protection of the frost-susceptible subgrade surface against freezing in the direction from the embankment slope and from the surface of the track bench. The use of extruded polystyrene boards is recommended in the design – see Figure 10.
 4. Due to the fact that each structural composition of the sub-ballast layers must be assessed for both traffic (design thickness of the sub-ballast layer – Figure 7) and non-traffic loads (design thickness of the protective subgrade surface layer – Figure 11), the greater design thickness determined from both assessment procedures is decisive. These findings thus imply that the greater thickness of the crushed aggregate layer will be used in the final design of the modified sub-ballast layers combined with a 150 mm thick foam glass aggregate layer.
 5. In terms of the assessment of the sub-ballast layers for non-traffic loads (design of the protective layer thickness), the increase of the design thickness of the foam glass aggregate layer from 150 mm to 200 mm allows a smaller design thickness of the crushed aggregate layer by 150 mm compared to the thickness of the protective layer determined by Figure 11. However, in many cases the designed crushed aggregate layer would have to be increased in size if such a structure were assessed for deformation resistance, particularly in cases where the deformation resistance of the subgrade surface is low, and therefore the benefit of increasing the thickness of the foam glass aggregate would be negligible. However, the design of a modified sub-ballast layers with a 200 mm thick foam glass aggregate layer would be of interest in the case of an air freezing index $I_F > 1200 \text{ }^\circ\text{C, day}$ and higher values of the deformation resistance of the subgrade surface.
 6. In the framework of further DRETM research activity, an assessment of the real thermal insulation effects of foam glass material incorporated in the railway track structure is considered from the perspective of the obtained results. At the same time, it is assumed that the possibility of applying foam glass boards to the structure of the sub-ballast layers will be assessed in the same way and then compared with the aggregate of 0/63 mm, the application of which was part of the analysis presented in this paper. It is also assumed that a comparison will be conducted with extruded polystyrene boards with the trade name 5000 CS.

Acknowledgements

Authors acknowledge, thank, and pay gratitude to the management of University of Zilina for their technical guidance and financial support during research work.

Funding

This work was supported by Grant System of University of Zilina No. 1/2021 (Number of project 12764) and the VEGA grant project 1/0084/20 Numerical and experimental analysis of transition areas of objects of structures of railway superstructures and objects of formation substructure.

Disclosure statement

No potential conflict of interest was reported by the authors.

References

- Arulrajah, A., Disfani, M. M., Maghoolpilehrood, F., Horpibulsuk, S., Udonchai, A., Imteaz, M., & Du, Y. J. (2015). Engineering and environmental properties of foamed recycled glass as a lightweight engineering material. *Journal of Cleaner Production*, 94, 369–375. <https://doi.org/10.1016/j.jclepro.2015.01.080>
- Bąk, A., & Chmielewski, R. (2019). The influence of fine fractions content in non-cohesive soils on their compactibility and the CBR value. *Journal of Civil Engineering and Management*, 25(4), 353–361. <https://doi.org/10.3846/jcem.2019.9687>
- Bian, J., Cao, W., Yang, L., & Xiong, C. (2018). Experimental research on the mechanical properties of tailing microcrystalline foam glass. *Materials*, 11(10), 2048. <https://doi.org/10.3390/ma11102048> <https://doi.org/10.3846/jcem.2019.9687>
- Buša, J., Pirč, V., & Schrötter, Š. (2006). *Numerical methods, probability and mathematical statistics*. Košice, Slovak Republic (in Slovak). <http://web.tuke.sk/fei-km/sites/default/files/prilohy/1/statnumo.pdf>
- Directorate General of Railways of the Slovak Republic. (2005). *The design of structural layers of subgrade structures* (TNŽ 73 6312) (in Slovak).
- Directorate General of Railways of the Slovak Republic. (2018). *Slovak railway regulation TS4 „Track substructure – Appendix 6“* (in Slovak).
- Esveld, C., & Markine, V. L. (2003, August). Use of expanded polystyrene (EPS) sub-base in railway track design. In *IABSE Symposium: Structures for High-Speed Railway Transportation* (pp. 252–253). Antwerpen, Belgium. <https://doi.org/10.2749/222137803796329952>
- Fredlund, M., & Haihua, L. (2011). *ACUMESH, 2D/3D Visualization software* (User's manual). Saskatoon, Saskatchewan, Canada.
- Frydenlund, T. E., & Aaboe, R. (2003). Foamglass – a new vision in road construction. In *22nd PIARC World Road Congress*. Durban, South Africa. <https://www.vegvesen.no/globalassets/fag/fokusomrader/forskning-innovasjon-og-utvikling/07-piarc-frydenlund-foamglass-a-new-vision-in-road-construction.pdf>
- Ghafari, N., Segui, P., Bilodeau, J. P., Cote, J., & Dore, G. (2019). Assessment of mechanical and thermal properties of foam glass aggregates for use in pavements. In *Proceedings of the 2019 TAC-ITS Canada Joint Conference*. Halifax, Canada. https://www.tac-atc.ca/sites/default/files/conf_papers/bilodeaujf-assessment_of_mechanical_and_thermal_properties_of_foam_glass_aggregate.pdf
- Glapor. (n.d.). *Cellular glass gravel*. <https://www.glapor.de/en/produkte/cellular-glass-gravel/>
- Gnip, I., Vėjelis, S., & Keršulis, V. (2001). The equilibrium moisture content of low-density thermal insulating materials. *Journal of Civil Engineering and Management*, 7(5), 359–365. <https://doi.org/10.3846/13921525.2001.10531754>
- Hisham, N. A. N., Zaid, M. H. M., Aziz, S. H. A., & Muhammad, F. D. (2021). Comparison of foam glass-ceramics with different composition derived from ark clamshell (ACS) and soda lime silica (SLS) glass bottles sintered at various temperatures. *Materials*, 14(3), 570. <https://doi.org/10.3390/ma14030570>
- Ižvolt, L., Dobeš, P., Drusa, M., Kadela, M., & Holesova, M. (2022). Experimental and numerical verification of the railway track substructure with innovative thermal insulation materials. *Materials*, 15(1), 160. <https://doi.org/10.3390/ma15010160>
- Ižvolt, L., Dobeš, P., & Mečár, M. (2013). Contribution to the methodology of the determination of the thermal conductivity coefficients λ of materials applied in the railway substructure. *Communications*, 15(4), 9–17. <https://doi.org/10.26552/com.C.2013.4.9-17>
- Ižvolt, L., Dobeš, P., & Mečár, M. (2019, September). Testing the suitability of the reinforced foam concrete layer application in the track bed structure. In *28th Russian – Polish – Slovak seminar. Theoretical Foundation of Civil Engineering*. Žilina, Slovakia. <https://doi.org/10.1088/1757-899X/661/1/012014>
- Ižvolt, L., Dobeš, P., & Mečár, M. (2020). Testing the suitability of the extruded polystyrene (Styrodur) application in the track substructure. *Acta Polytechnica*, 60(3), 243–251. <https://doi.org/10.14311/AP.2020.60.0243>
- Ižvolt, L., Dobeš, P., & Pieš, J. (2018). Verification of boundary conditions of numerical modeling of the track substructure thermal regime – influence of the snow cover. *Archives of Transport*, 48(4), 51–60. <https://doi.org/10.5604/01.3001.0012.8365>
- Ižvolt, L., Dobeš, P., Holešová, M., & Navikas, D. (2021). Numerical modelling of thermal regime of railway track – structure with thermal insulation (Styrodur). *Journal of Civil Engineering and Management*, 27(7), 525–538. <https://doi.org/10.3846/jcem.2021.14903>
- Kitaygorodskiy, I. I. (1932). *Transactions of the All-Union Conference on Standardization and Production of New Construction Materials*. Moscow.
- Lenart, S., & Kaynia, A. M. (2019). Dynamic properties of lightweight foamed glass and their effect on railway vibration. *Transportation Geotechnics*, 21, 100276. <https://doi.org/10.1016/j.trgeo.2019.100276>
- Li, T.-f., Chen, F., Li, Z.-G., Wilk, S., & Basye, C. (2020). *Lightweight foamed concrete subgrade for heavy haul railway*. Geosynthetica. <https://www.geosynthetica.com/lightweight-foamed-concrete-subgrade-railways>
- Loranger, B., Kuznetsova, E., Hoff, I., Aksnes, J., & Skoglund, K. A. (2017). Evaluation of Norwegian gradation based regulation for frost susceptibility of crushed rock aggregates in roads and railways. In A. Loizos, I. Al-Qadi, & T. Scarpas (Eds.), *Bearing capacity of roads, railways and airfields* (pp. 2077–2085). CRC Press. <https://doi.org/10.1201/9781315100333-275>
- Lu, J., & Onitsuka, K. (2004). Construction utilization of foamed waste glass. *Journal of Environmental Sciences*, 16(2), 302–307.
- Morgan, J. S., Wood, J. L., & Bradt, R. C. (1981). Cell size effects on the strength of foamed glass. *Materials Science and Engineering*, 47(1), 37–42. [https://doi.org/10.1016/0025-5416\(81\)90038-0](https://doi.org/10.1016/0025-5416(81)90038-0)
- Nurmikolu, A., & Kolisoja, P. (2005). Extruded polystyrene (XPS) foam frost insulation boards in railway structures. In *Proceedings of the 16th International Conference on Soil Mechanics and Geotechnical Engineering* (pp. 1761–1764). Osaka, Japan. <https://doi.org/10.3233/978-1-61499-656-9-1761>
- Paunescu, L., Axinte, S. M., Dragoescu, M. F., & Cosmulescu, F. (2021). Adequate correlation between the physical and mechanical properties of glass foam. *Journal La Multiapp*, 2(4), 14–26. <https://doi.org/10.37899/journallamultiapp.v2i4.415>
- Pieš, J., & Mócová, L. (2019, May). Application of TDR test probe for determination of moisture changes of railway substructure materials. In *Proceedings of the 13th International Scientific Conference on Sustainable, Modern and Safe Transport (TRANSCOM 2019)*. Nový Smokovec, Slovak Republic. <https://doi.org/10.1016/j.trpro.2019.07.013>
- Qin, Z., Li, G., Tian, Y., Ma, Y., & Shen, P. (2019). Numerical simulation of thermal conductivity of foam glass based on the steady-state method. *Materials*, 12(1), 54. <https://doi.org/10.3390/ma12010054>

- Republic of Slovenia Statistical Office. (2018). *European mobility week*. <https://www.stat.si/StatWeb/en/News/Index/9805>
- Sadrinezhad, A., Tehrani, F. M., & Jeevanlal, B. (2019, March). Shake table test of railway embankment consisting of TDA and LECA. In *Eighth International Conference on Case Histories in Geotechnical Engineering (Geo-Congress 2019)* (pp. 31–39). Philadelphia, Pennsylvania, United States. <https://doi.org/10.1061/9780784482100.004>
- Slovak Office of Standards, Metrology and Testing. (2017). *Road building. Roads embankments and subgrades* (STN 73 6133). Slovak Republic (in Slovak).
- Styrodur. (2019). *Load-bearing and floor insulation*. <https://www.styrodur.com/portal/streamer?fid=1225078>
- Thode, R. (2012). *SVHEAT, 2D/3D geothermal modeling software. Tutorial manual*. Saskatoon, Saskatchewan, Canada. <https://manualzilla.com/doc/5907794/svheat-tutorial-manual>
- Vlček, J., & Valášková, V. (2021). Determination of the deformation characteristics of the foam concrete as a sub-base. *Journal of Vibroengineering: Theoretical & Practical Aspects of Vibration Engineering*, 23(1), 156–166. <https://doi.org/10.21595/jve.2020.21108>
- Woodward, P. K., El Kacimi, A., Laghrouche, O., Medero, G., & Benumahd, M. (2012). Application of polyurethane geocomposites to help maintain track geometry for high-speed ballasted railway tracks. *Journal of Zhejiang University SCIENCE A*, 13(11), 836–849. <https://doi.org/10.1631/jzus.A12ISGT3>